Search for WH associated production in 5.3 fb^{-1} of $p\bar{p}$ collisions at the Fermilab Tevatron: Supplementary material

The D0 Collaboration
(Dated: December 6, 2010)

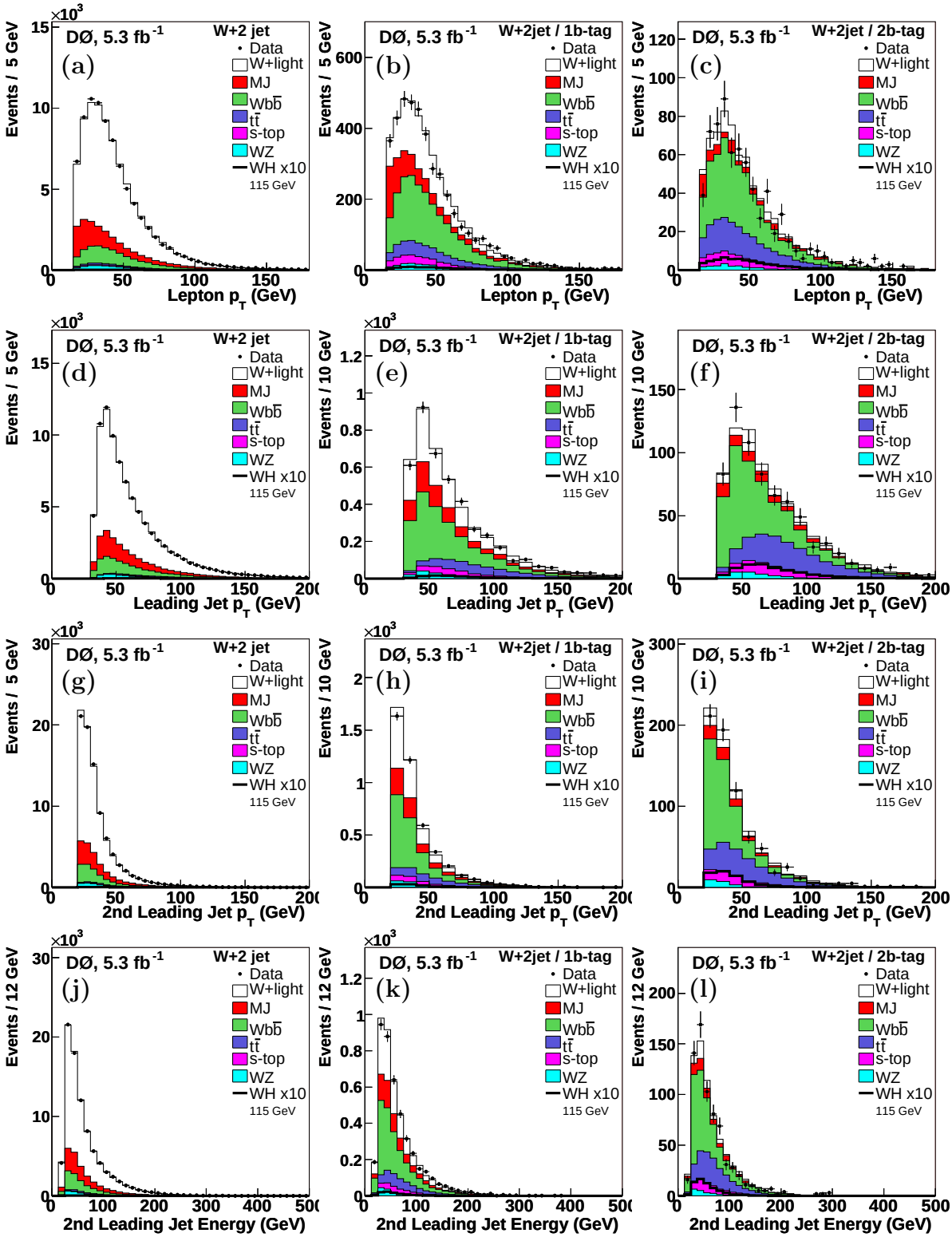

FIG. 1: Distribution in the W+2-jets sample of the observed (a-c) lepton p_T, (d-f) leading jet p_T, (g-i) 2nd leading jet p_T, and (j-l) 2nd leading jet energy in data compared to the simulated expectation. The left, center and right columns show pre-b-tagged, ST and DT data, respectively. The simulation is normalized to the integrated luminosity of the data sample using the expected cross sections (absolute normalization) except for the W+jets sample which is normalized to the pre-b-tagged data.

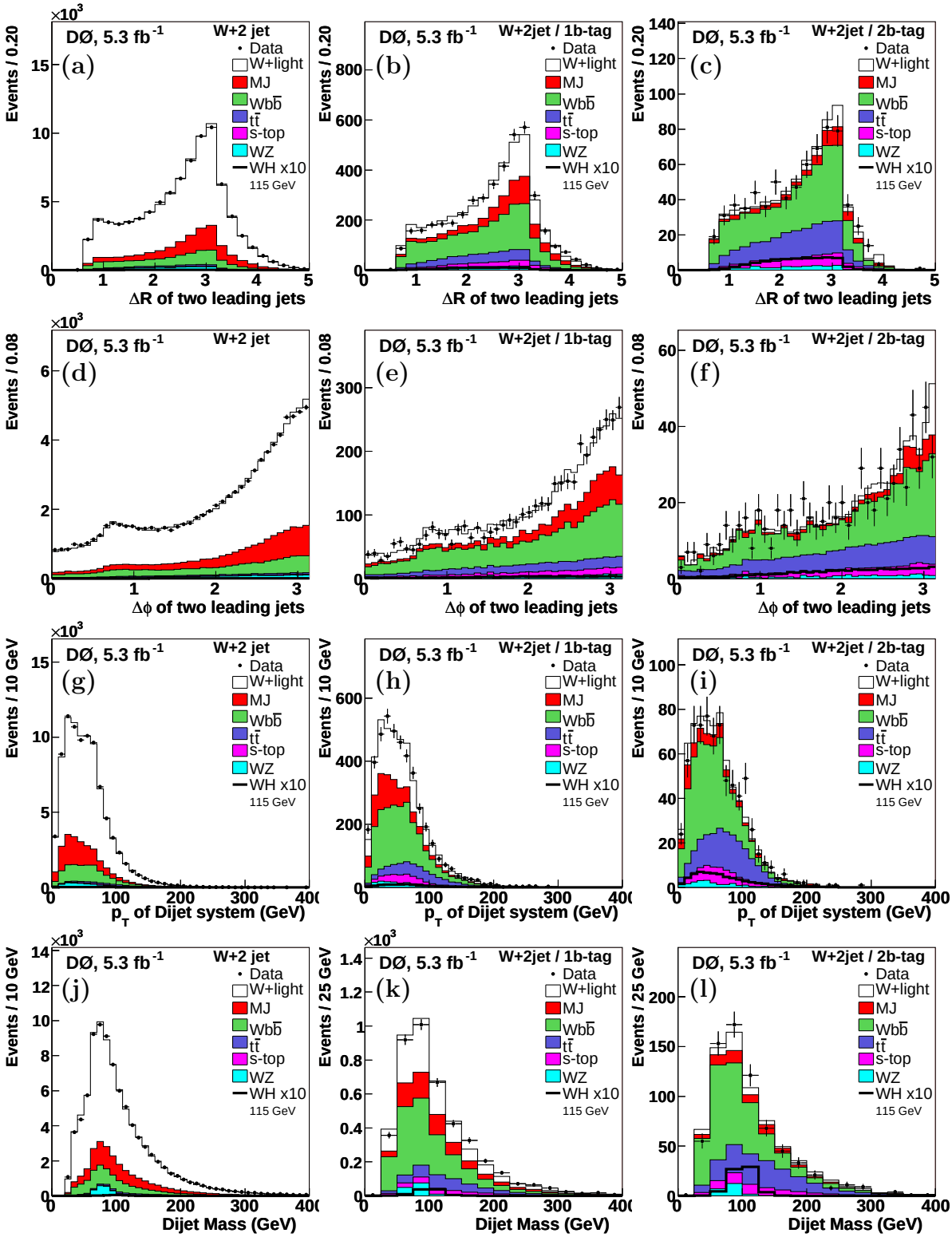

FIG. 2: Distribution in the W+2-jets sample of the observed (a-c) $\Delta\mathcal{R}$(two leading jets), (d-f) $\Delta\phi$(two leading jets), (g-i) p_T(dijet system), and (j-l) dijet invariant mass in data compared to the simulated expectation. The left, center and right columns show pre-b-tagged, ST and DT data, respectively. The simulation is normalized to the integrated luminosity of the data sample using the expected cross sections (absolute normalization) except for the W+jets sample which is normalized to the pre-b-tagged data.

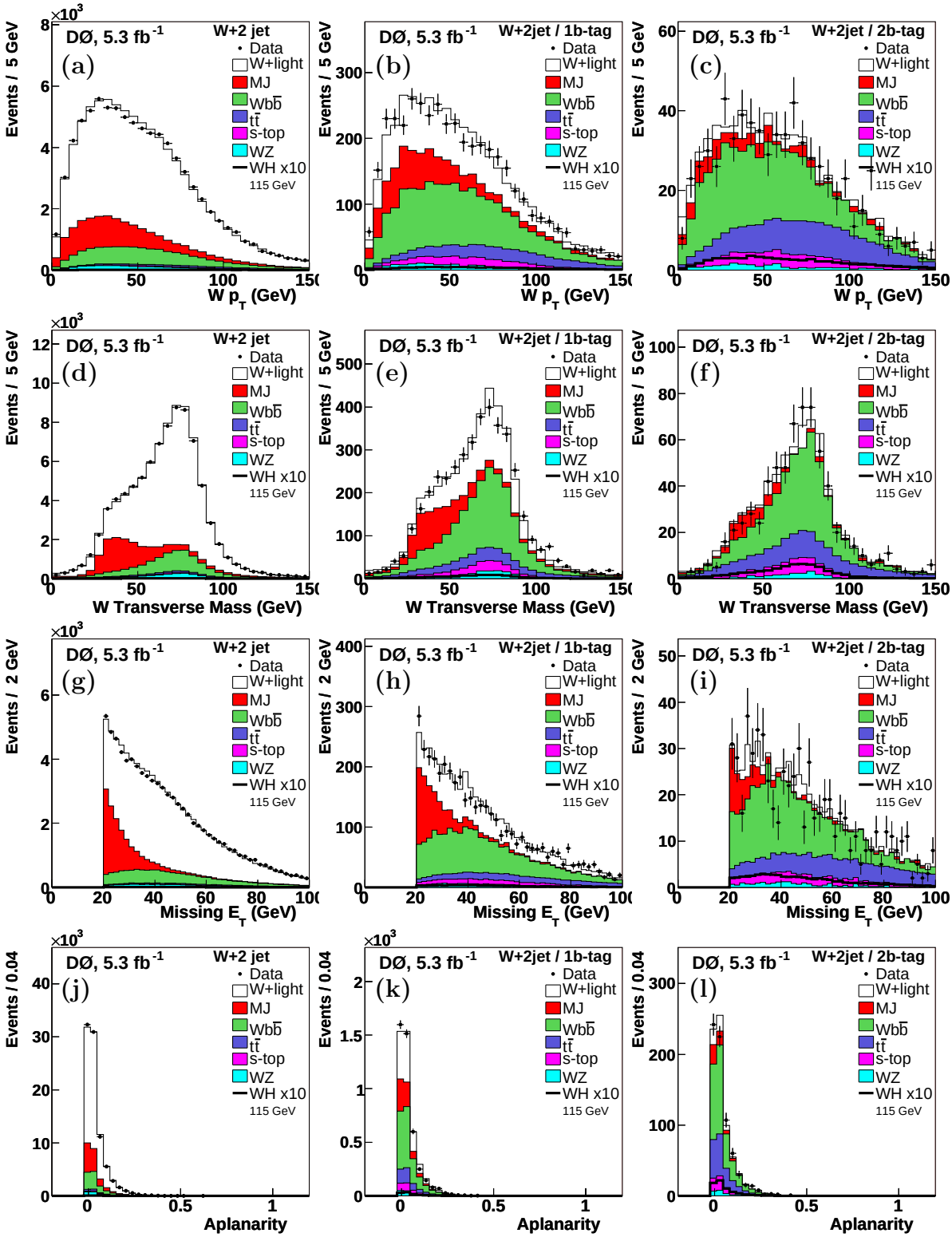

FIG. 3: Distribution in the W+2-jets sample of the observed (a-c) $p_T(\ell$-$\not\!\!E_T$ system), (d-f) transverse mass of ℓ-$\not\!\!E_T$ system, (g-i) $\not\!\!E_T$, and (j-l) aplanarity in data compared to the simulated expectation. The left, center and right columns show pre-b-tagged, ST and DT data, respectively. The simulation is normalized to the integrated luminosity of the data sample using the expected cross sections (absolute normalization) except for the W+jets sample which is normalized to the pre-b-tagged data.

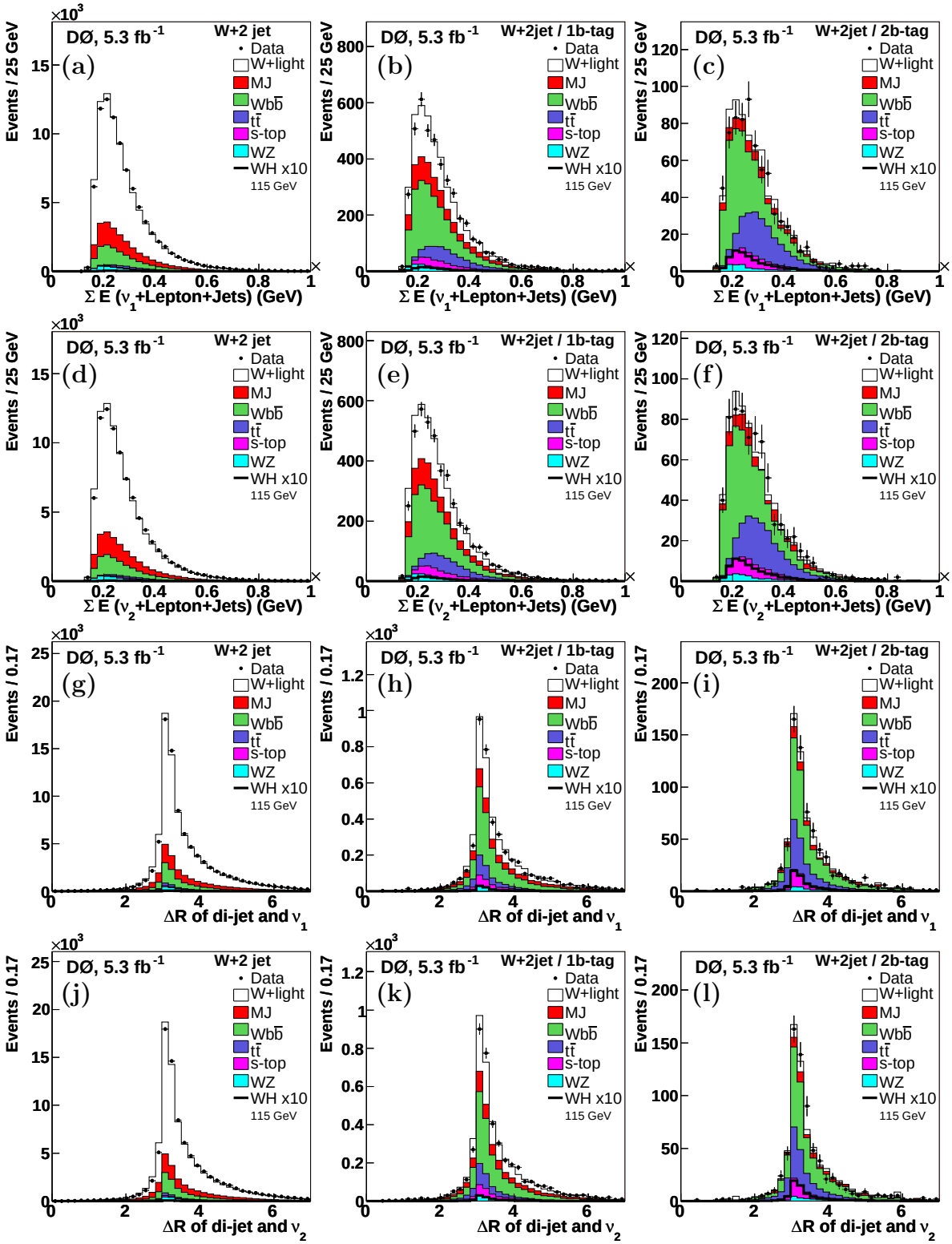

FIG. 4: Distribution in the W+2-jets sample of the observed (a-c) $\sqrt{\hat{s}}$ (ν p_Z solution 1), (d-f) $\sqrt{\hat{s}}$ (ν p_Z solution 2), (g-i) $\Delta\mathcal{R}$(dijet system, ℓ-ν system) (ν p_Z solution 1), and (j-l) $\Delta\mathcal{R}$(dijet system, ℓ-ν system) (ν p_Z solution 2) in data compared to the simulated expectation. The left, center and right columns show pre-b-tagged, ST and DT data, respectively. The simulation is normalized to the integrated luminosity of the data sample using the expected cross sections (absolute normalization) except for the W+jets sample which is normalized to the pre-b-tagged data.

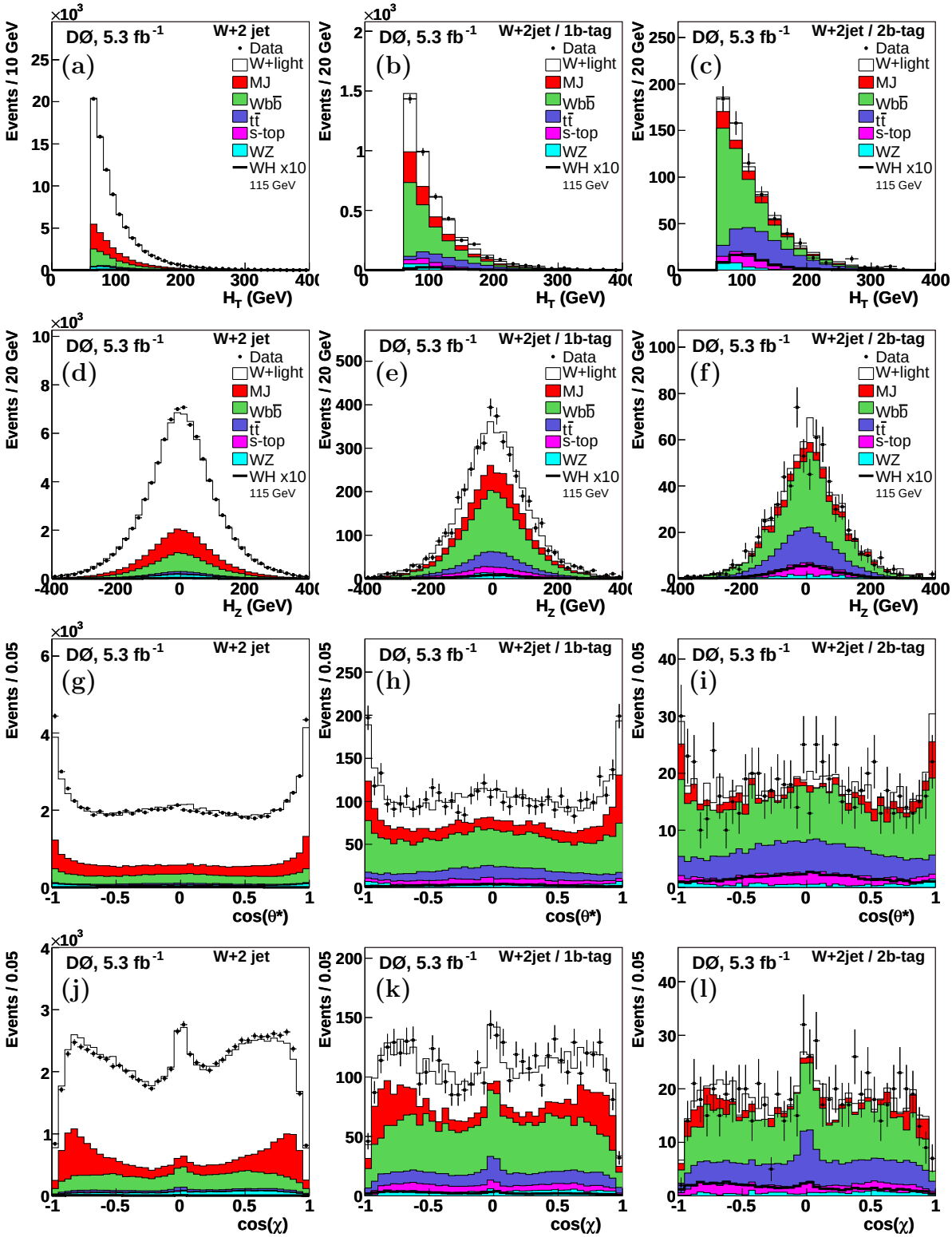

FIG. 5: Distribution in the W+2-jets sample of the observed (a-c) H_T, (d-f) H_Z, (g-i) $\cos\theta^*$, and (j-l) $\cos\chi$ in data compared to the simulated expectation. The left, center and right columns show pre-b-tagged, ST and DT data, respectively. The simulation is normalized to the integrated luminosity of the data sample using the expected cross sections (absolute normalization) except for the W+jets sample which is normalized to the pre-b-tagged data.

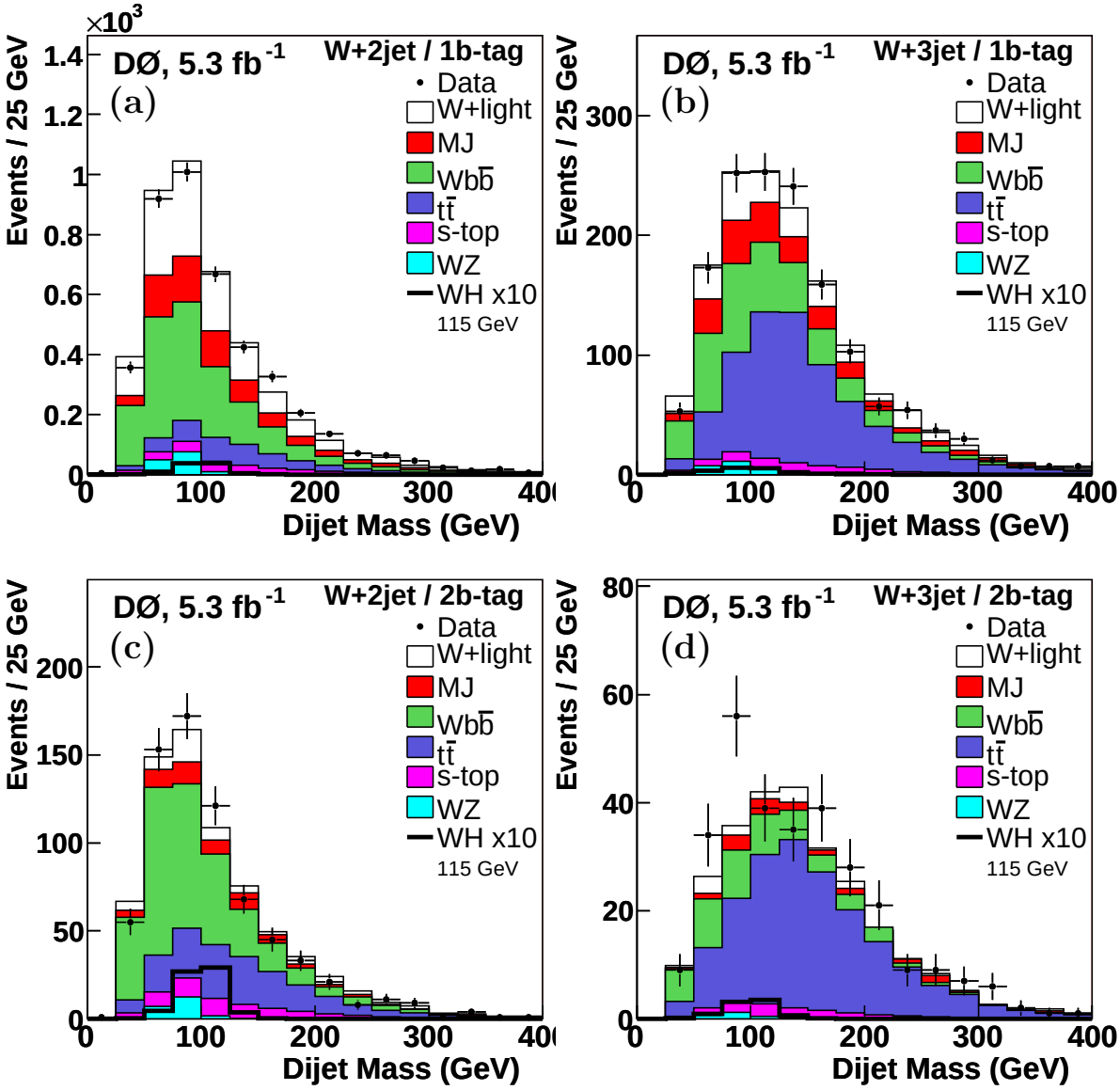

FIG. 6: Dijet invariant mass in (a) W+2-jets and (b) W+3-jets events when exactly one jet is b-tagged and in (c) W+2-jets and (d) W+3-jets events when at least 2 jets are b-tagged. The simulation is normalized to the integrated luminosity of the data sample using the expected cross sections (absolute normalization) except for the W+jets sample which is normalized to the pre-b-tagged data.

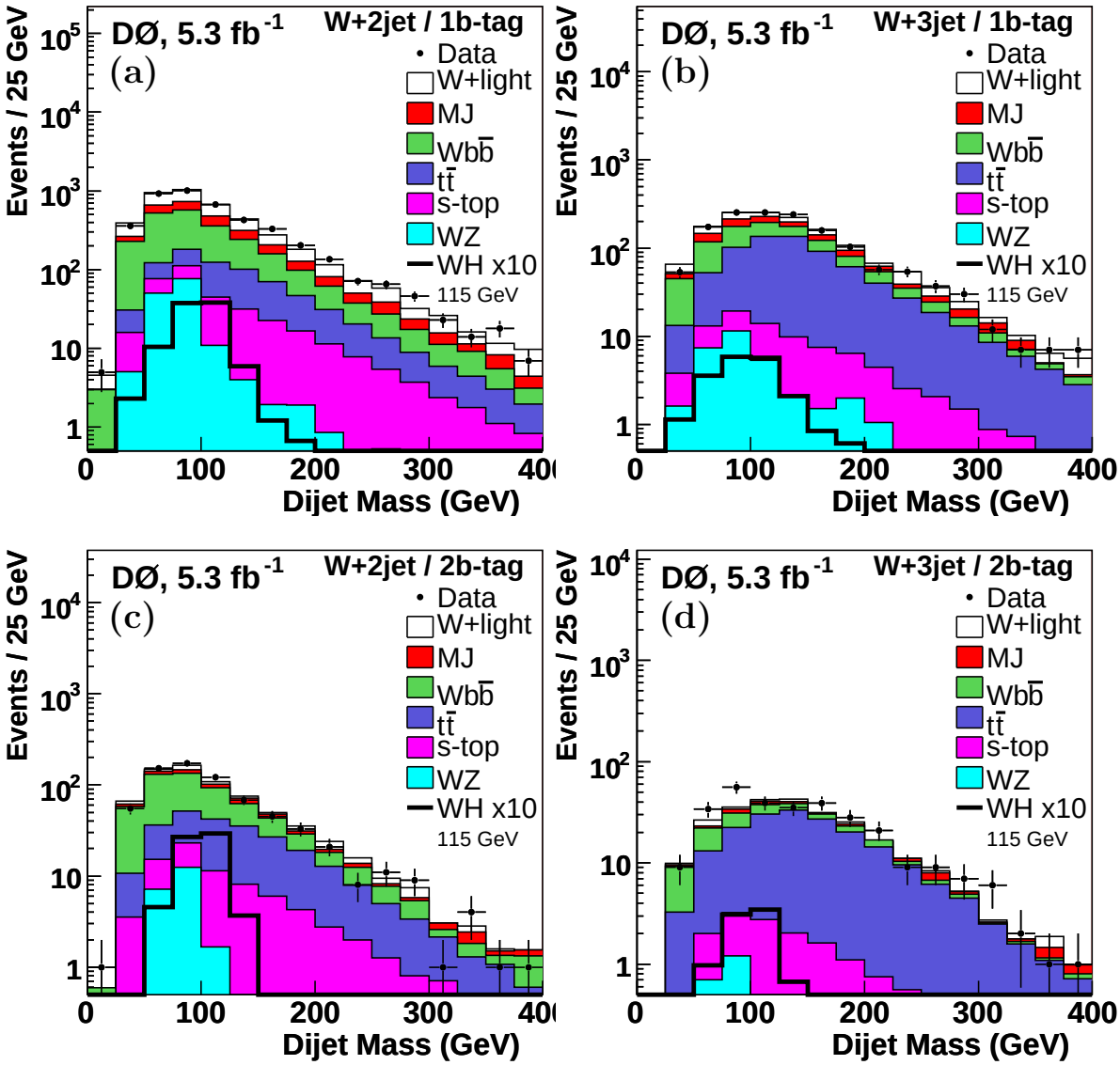

FIG. 7: Dijet invariant mass in (a) W+2-jets and (b) W+3-jets events when exactly one jet is b-tagged and in (c) W+2-jets and (d) W+3-jets events when at least 2 jets are b-tagged, in logarithmic scale. The simulation is normalized to the integrated luminosity of the data sample using the expected cross sections (absolute normalization) except for the W+jets sample which is normalized to the pre-b-tagged data.

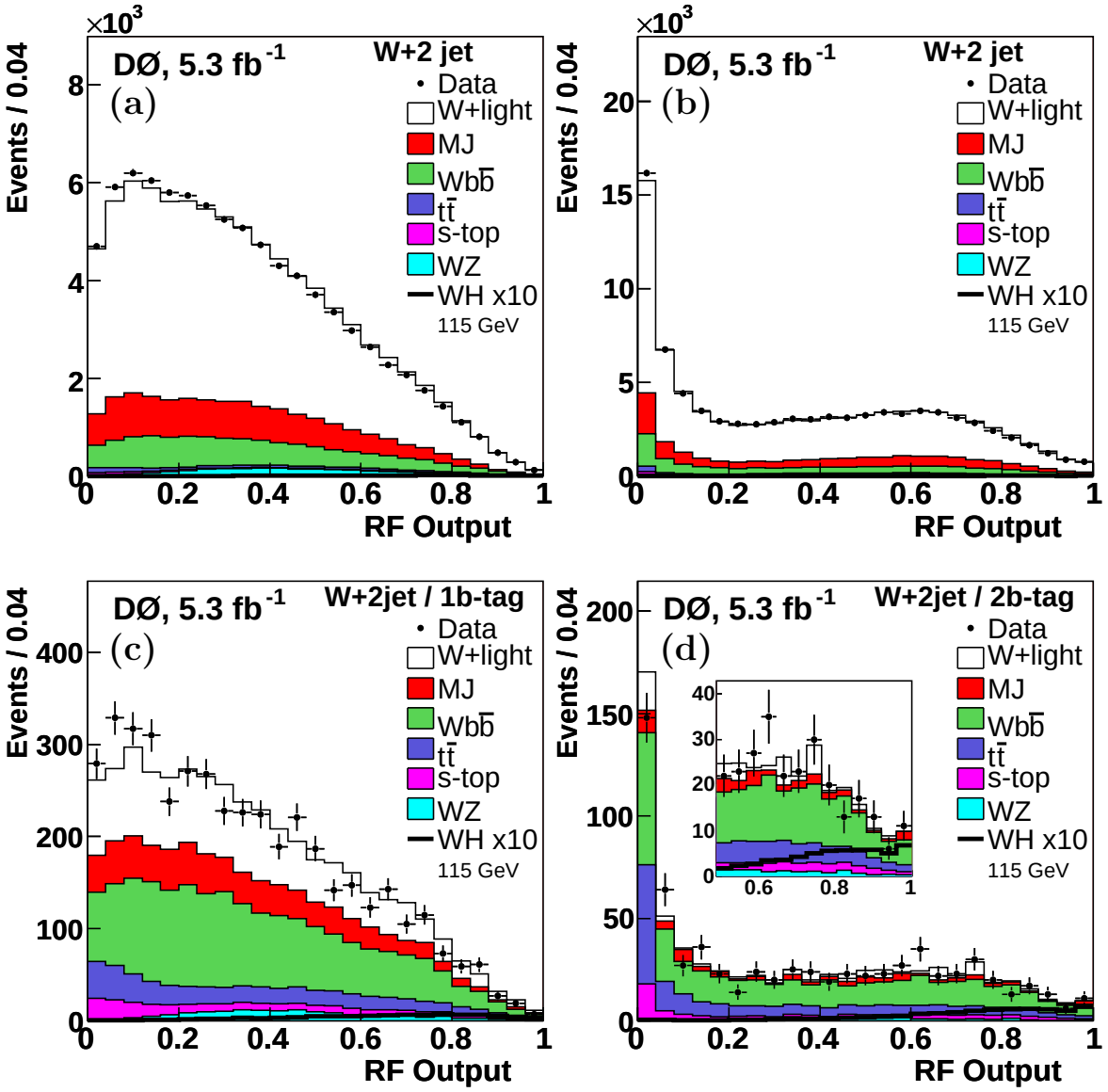

FIG. 8: Distributions (with linear vertical scale) of the W+2-jets RF output compared with the simulated expectation: (a) before b-tagging for the ST RF; (b) before b-tagging for the DT RF; (c) in the single $b-$tag sample for the ST RF; (d) in the double $b-$tag sample for the DT RF. The simulation is normalized to the integrated luminosity of the data sample using the expected cross sections (absolute normalization) except for the W+jets sample which is normalized to the pre-b-tagged data.

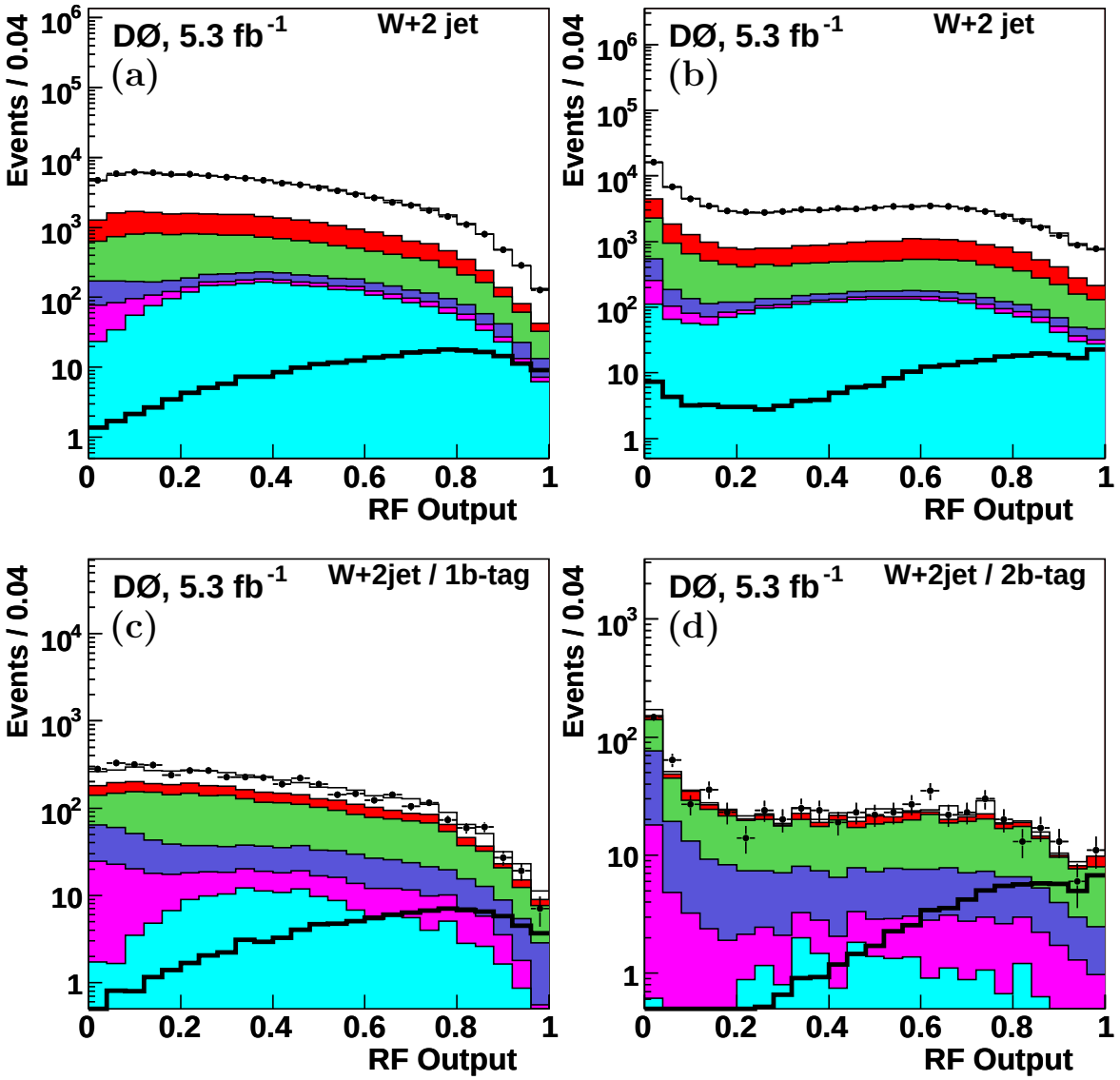

FIG. 9: Distributions (with logarithmic vertical scale) of the W+2-jets RF output compared with the simulated expectation: (a) before b-tagging for the ST RF; (b) before b-tagging for the DT RF; (c) in the single $b-$tag sample for the ST RF; (d) in the double $b-$tag sample for the DT RF. The simulation is normalized to the integrated luminosity of the data sample using the expected cross sections (absolute normalization) except for the W+jets sample which is normalized to the pre-b-tagged data.

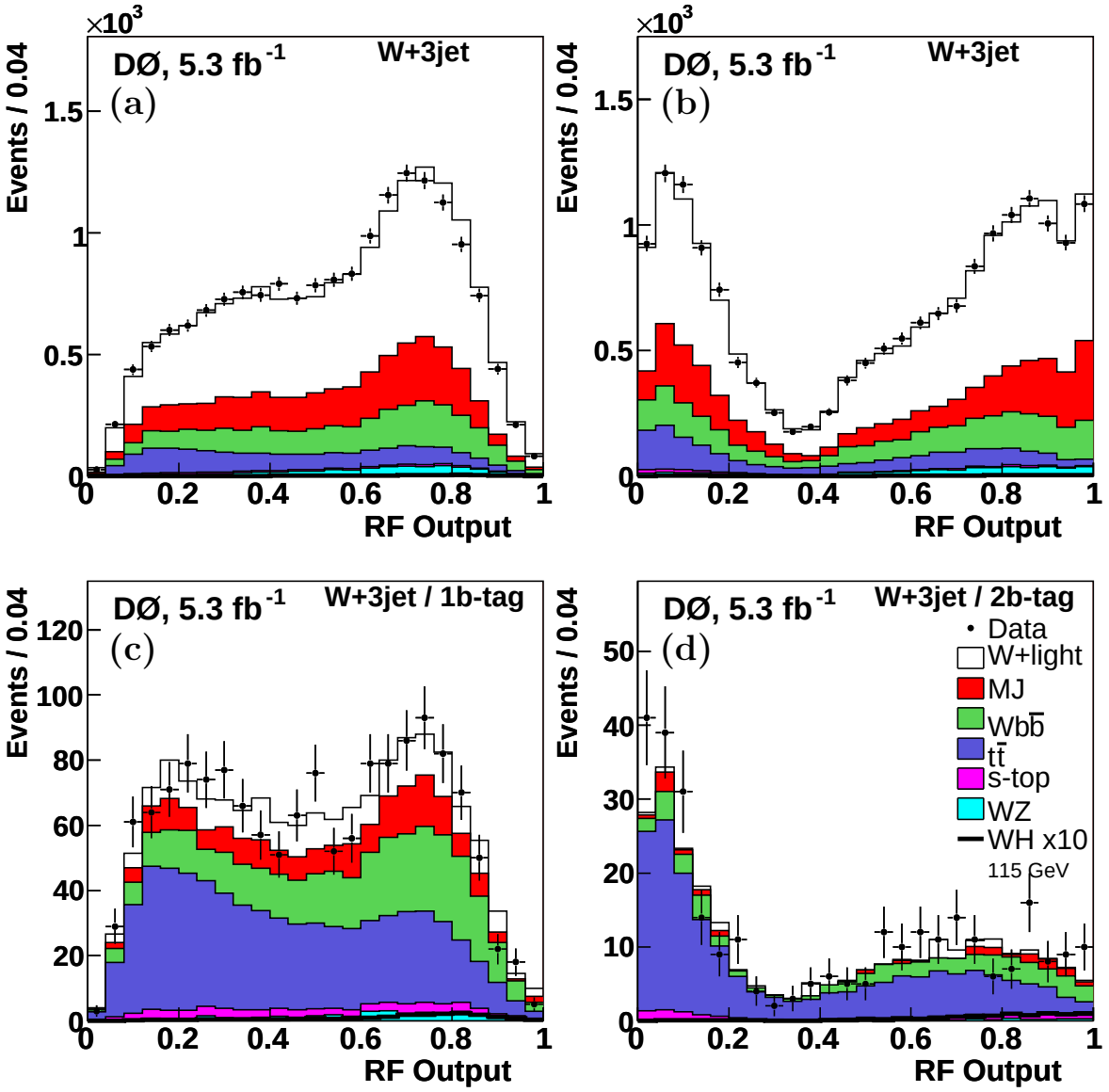

FIG. 10: Distributions (with linear vertical scale) of the W+3-jets RF output compared with the simulated expectation: (a) before b-tagging for the ST RF; (b) before b-tagging for the DT RF; (c) in the single $b-$tag sample for the ST RF; (d) in the double $b-$tag sample for the DT RF. The simulation is normalized to the integrated luminosity of the data sample using the expected cross sections (absolute normalization) except for the W+jets sample which is normalized to the pre-b-tagged data.

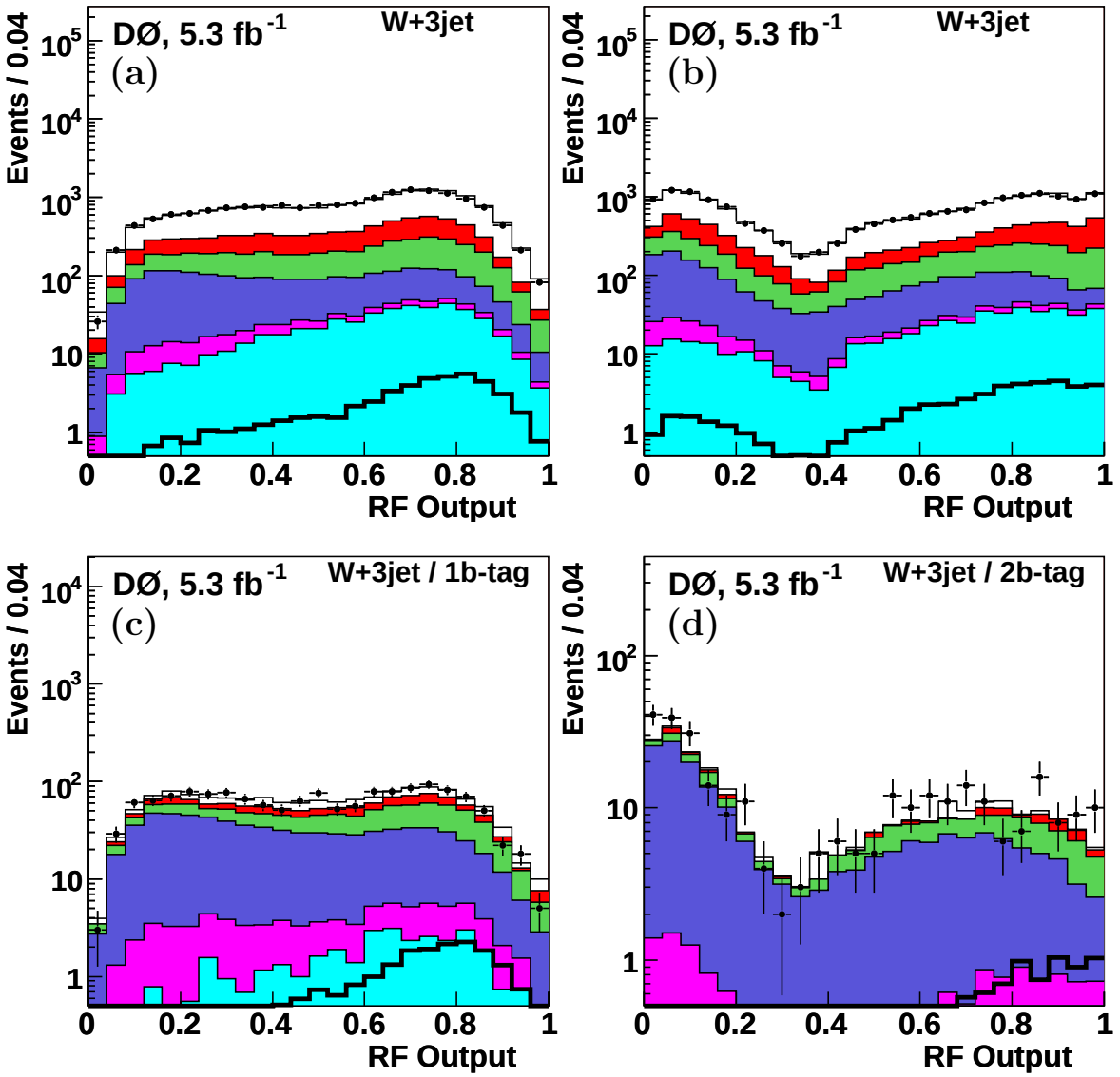

FIG. 11: Distributions (with logarithmic vertical scale) of the W+3-jets RF output compared with the simulated expectation: (a) before b-tagging for the ST RF; (b) before b-tagging for the DT RF; (c) in the single $b-$tag sample for the ST RF; (d) in the double $b-$tag sample for the DT RF. The simulation is normalized to the integrated luminosity of the data sample using the expected cross sections (absolute normalization) except for the W+jets sample which is normalized to the pre-b-tagged data.